



## An alternative approach to model the Internal Activity of integrated circuits

Nestor Berbel, Raul Fernandez-Garcia, Ignacio Gil, Binhong Li, Sonia Ben Dhia, Alexandre Boyer

### ► To cite this version:

Nestor Berbel, Raul Fernandez-Garcia, Ignacio Gil, Binhong Li, Sonia Ben Dhia, et al.. An alternative approach to model the Internal Activity of integrated circuits. 8th Workshop on Electromagnetic Compatibility of Integrated Circuits, Nov 2011, Dubrovnik, Croatia. pp.88. hal-00669719

HAL Id: hal-00669719

<https://hal.science/hal-00669719>

Submitted on 13 Feb 2012

**HAL** is a multi-disciplinary open access archive for the deposit and dissemination of scientific research documents, whether they are published or not. The documents may come from teaching and research institutions in France or abroad, or from public or private research centers.

L'archive ouverte pluridisciplinaire **HAL**, est destinée au dépôt et à la diffusion de documents scientifiques de niveau recherche, publiés ou non, émanant des établissements d'enseignement et de recherche français ou étrangers, des laboratoires publics ou privés.

# An alternative approach to model the Internal Activity of integrated circuits.

N. Berbel, R. Fernández-García, I. Gil

Departament d'Enginyeria Electrònica  
UPC Barcelona Tech  
Terrassa, SPAIN  
nestor.berbel-ortal@upc.edu

B. Li, S. Ben-Dhia, A. Boyer

Departament de Génie Électrique et Informatique  
LAAS-CNRS, INSA de Toulouse  
Toulouse, France

**Abstract**—This paper deals with the EMC modeling of integrated circuits and the standardized model IEC 62433-2 (Integrated Circuit Emission Model – Conducted Emission [1]). This standardized model has been applied into a basic digital circuit: a ring oscillator. This work presents an alternative approach to model and quantify the Internal Activity of any digital or analog integrated circuit, and its use has been applied on the ring oscillator.

**Keywords:** ICEM-CE, integrated circuit, EMC, internal activity.

## I. INTRODUCTION

Electromagnetic compatibility (EMC) problem has been studied for many years, especially at printed circuit board (PCB) level [2]. Due to the increase of complexity and miniaturization of microelectronic components, rising frequencies and bitrates, a demand to characterize the EMC at Integrated Circuits (IC) level has increased. In fact, nowadays the electronics industry requires electrical models to predict conducted or radiated emissions [3], signal and power integrity at IC level [4].

Several models have been created to predict the conducted emissions. For example the Linear Equivalent Circuit and Current Source (LECCS) model [5] has been used for prediction of conducted and radiated emissions and for immunity tests. The International Electro-technical Commission (IEC) has standardized another model to predict the conducted electromagnetic emissions at IC: the international directive IEC 62433-2 or Integrated Circuit Emission Model – Conducted Emissions (ICEM-CE) [1].

The ICEM-CE model has been used in several works: to solve the decoupling capacitor of an ASIC IC [6], to perform a jitter analysis of an integrated phase-locked loop [7], to model the electromagnetic emission of a microcontroller [8] and to estimate the effect of Digital Signal Controllers disturbances on measurements and control systems [9].

The ICEM-CE models the switching noise of the IC like a current source, with its data typically described by an internal activity (IA) loaded on an ASCII format. The IA is described in frequency domain (frequency harmonics and its amplitude) or in time domain (time and the amplitude of the signal at each time). Usually, a simple waveform such a triangular waveform can be used for the component description.

By modeling the IA with an ASCII file, it is difficult to quantify the variation in the IA. On the other hand, with a triangular waveform, a good correlation between the IA model and the IA measurement is not achieved. In this paper, an alternative approach to model the switching noise is proposed, which avoid the aforementioned limitations. This alternative modeling of the IA is based on the analysis of its spectral components and it is presented in order to quantify the impact of several effects on the different harmonics of the internal activity. The proposed IA model is verified with a Digital Ring Oscillator, integrated on a 64 Led Plastic Thin-Quad Flatpack (TQFP) package.

The paper is organized as follows: In Section II, the ICEM-CE model is presented, detailing each part and how it is obtained experimentally. In Section III, the alternative model for the IA is presented and detailed. In Section IV, experimental results are shown. Finally, in Section V, conclusions are summarized.

## II. ICEM-CE MODEL

In order to predict the impact of the electromagnetic interference (EMI) on the electronic systems performance, electrical circuit models, which take into account EMI, are required. In this sense, an electromagnetic model of integrated circuits has been standardized (ICEM-CE model). This model includes a passive distribution network (PDN) and the internal activity (IA). The ICEM-CE model is depicted on Fig. 1.

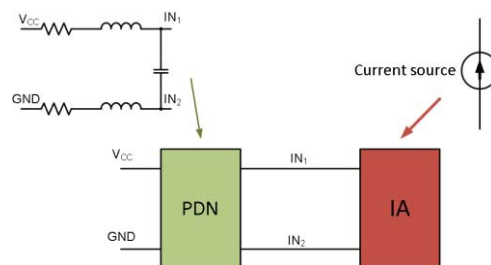


Figure 1: ICEM-CE model

This work has been supported by the Spain-MICINN under Project TEC2010-18550 and AGAUR 2009 SGR 1425. The authors want to thank to B. Vrignon from Freescale Semiconductors for sample provision.

#### A. Passive Distribution Network (PDN).

The Passive Distribution Network (PDN) presents the characteristics of the propagation paths of electromagnetic noise. These propagation paths are modeled with passive components, inductors, capacitors and resistors, which values are measured by performing a two-port self-impedance measurement [1] and by obtaining the  $S_{21}$  scattering parameter. Then, the input impedance,  $Z_{in}$ , is calculated and the PDN is extracted.

#### B. Internal Activity (IA).

The Internal Activity (IA) models the switching noise of the integrated circuits, measured according to the schematic presented on Fig. 2 [1]. The ground terminal of the integrated circuit is connected to a  $1\ \Omega$  resistor, which is used to measure the external current injected by the power supply. A  $49\ \Omega$  resistor is added in series with the instrument in order to provide a  $50\ \Omega$  equivalent impedance from the measurement instrument. The internal activity must be de-embedded from the emission current measured at the ground pin of the chip,  $I_E(t)$ , so as to obtain the switching noise of the integrated circuit.

The de-embedding process is detailed on Fig. 3. From the oscilloscope measurement ( $V_{EXT}(t)$ ) the external current is extracted ( $I_E(t)$ ). Since the external current is in time domain, Fast Fourier Transform (FFT) has to be performed in order to express the external current in frequency domain. The FFT is performed using a flat window. With the frequency response of the PDN, and the external current in frequency domain, the internal activity ( $I_A(f)$ ) is calculated by multiplying the frequency response of the PDN with the frequency response of the external current  $I_E(f)$ . The Inverse Fourier Transform of  $I_A(f)$  is performed to obtain the internal activity in time domain ( $I_A(t)$ ).

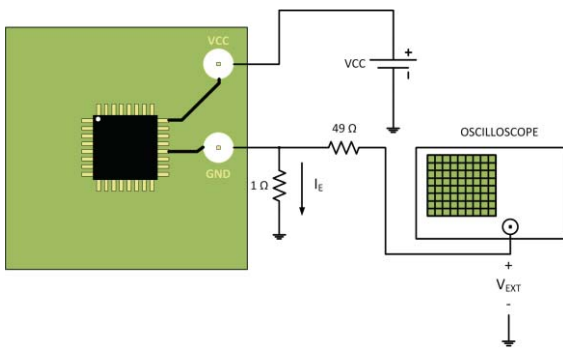


Figure 2: Set-up for measuring the Internal Activity

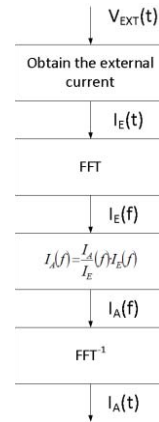


Figure 3: Process involved to model  $I_A(t)$

### III. ALTERNATIVE MODEL FOR THE INTERNAL ACTIVITY

Due to the limitations of the actual IA model presented on Section I, we present a model based on the spectral components of the periodic IA, described by means of equation (1). This alternative model expresses the IA as a sum of the first  $N_{HARM}$  even and odd harmonics of the IA. For each harmonic, its amplitude, frequency and phase are extracted and then the IA in time domain is computed.

$$I_A(t) = I_A|_{DC} + \sum_{n=1}^{N_{HARM}} A_n \cdot \cos(2 \cdot \pi \cdot f_n \cdot t + \varphi_n) \quad (1)$$

The number of harmonics  $N_{HARM}$  is chosen with the purpose to fit the measurements or the simulated data. The main advantage of this alternative model consists of the fact that the variations on the IA can be quantified for each harmonic and compared with the fresh devices. Moreover, a Spice model of the IA, which takes into account these variations, can be easily built in any electrical simulation tool by means of sinusoidal current sources.

### IV. EXPERIMENTAL RESULTS

To verify this alternative IA model, the ICEM-CE model of a ring oscillator has been extracted. The ring oscillator is built with 90 inverters and 1 NAND gate, with one ENABLE pin. The nominal oscillation frequency is 75 MHz at a nominal power supply of 1,2 V. The inverters and the NAND are built with 90 nm technology with a length and width channel of the transistors detailed on Table I. Fig. 4 shows the printed circuit board in which the measurement have been obtained.

TABLE I. SIZE OF THE TRANSISTORS USED ON THE RING OSCILLATOR

Transistor type	Size
NMOS	$L=0,1\ \mu\text{m} / W=0,23\ \mu\text{m}$
PMOS	$L=0,1\ \mu\text{m} / W=0,46\ \mu\text{m}$

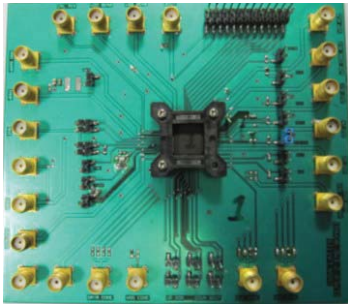


Figure 4: Printed circuit board of the ring oscillator.

The first step to obtain the ICEM-CE model is to extract the PDN, which is measured by using a Vector Network Analyzer (VNA). Fig. 5 shows the good correlation between the measurements and the model of the input impedance of the PDN extracted in the frequency range from 150 kHz to 1 GHz. Fig. 6 plots the completed PDN model and Table II summarizes the values of the PDN components. The components  $L_1$ ,  $R_1$ ,  $L_2$ ,  $R_2$ ,  $L_3$ ,  $R_3$ ,  $L_4$ ,  $R_4$  and  $C_1$  are related with PCB trace whereas  $L_5$ ,  $R_5$  and  $C_4$  are related with TQFP package. The components  $C_2$  and  $C_3$  correspond to the decoupling capacitors. The capacitor  $C_2$  and  $C_3$  are considered ideal, and also the 1  $\Omega$  measurement resistor is not taken into account in the PDN, which will lead to a high frequency discrepancy between the measurements and the electric model.

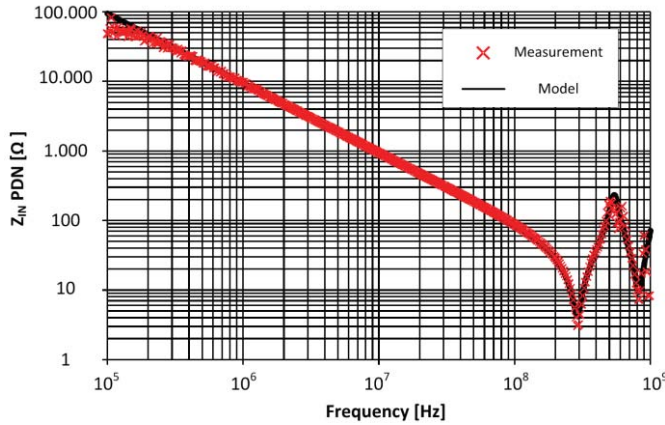


Figure 5: PDN input impedance.

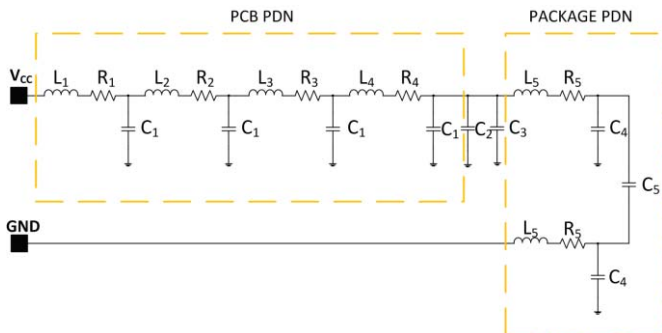


Figure 6: Passive Distribution Network of the Ring Oscillator.

TABLE II. VALUES OF THE PDN COMPONENTS

Component	Value
$L_1$	3,3 nH
$L_2$	4,9 nH
$L_3$	7,6 nH
$L_4$	6,19 nH
$L_5$	7 nH
$C_1$	2,5 pF
$C_2$	10 nF
$C_3$	100 nF
$C_4$	0,86 pF
$C_5$	5,9 pF
$R_1$	0,14 $\Omega$
$R_2$	0,276 $\Omega$
$R_3$	0,138 $\Omega$
$R_4$	0,1525 $\Omega$
$R_5$	5,2 $\Omega$

The IA of the ring oscillator is obtained by measuring the  $V_{EXT}$  voltage with the oscilloscope by performing the de-embedding process, detailed on Fig. 3. Fig. 7 shows the external current ( $I_E(t)$ ) measured with the oscilloscope for the supply voltages 1 V and 1,8 V. Fig. 8 plots the oscillation frequency of the RO for several supply voltages, which indicates that the frequency of the RO increases as the power supply increases. On Fig. 9, the frequency spectrum of the external current  $I_E$  is plotted for several supply voltages, 1 V and 1,8 V. Fig. 9 shows that the number of harmonics of  $I_E$  decreases as the power supply increases, meanwhile the first harmonic shifts its frequency, from 50 MHz to 140 MHz.

Figs. 10 and 11 shows the frequency spectrum of the internal activity once the de-embedding process has been carried out. With the IA de-embedded, a specific number of harmonics has to be chosen in order to fit the alternative IA model and the measurements. For a power supply voltage of 1 V, the 12 first even and odd harmonics have been taken into account. With these 12 first harmonics, a good correlation between the measurement and the alternative IA model is achieved. On the other hand, for a supply voltage of 1,8 V, to reach the same goal, 7 even and odd harmonics are taken into account for the proposed model. The information subtracted from the IA frequency spectrum is the amplitude, the frequency and the phase from each harmonic. Figs. 12 and 13 show the IA time domain signal, both the measurement and the model. As it can be seen, a good correlation between the measurements and the proposed model has been achieved for  $V_{CC}$  equal to 1 V and for  $V_{CC}$  equal to 1,8 V.

Finally, Fig. 14 plots the frequency,  $f_n$  parameter of equation (1), comparison for each harmonic of the IA at different power supply voltages. It can be concluded that an increase in the power supply produces an increase in the frequency of each harmonic, due to the increase of the frequency oscillation of the ring oscillation. Fig. 15 shows the amplitude for each harmonic, which presents a trend to increase, due to the switching noise levels increments as the power supply increases its value. Fig. 16 plots the phase for each harmonic, for 1 V and 1,8 V supply voltage. This information was needed to fit the alternative IA model and the measurements.

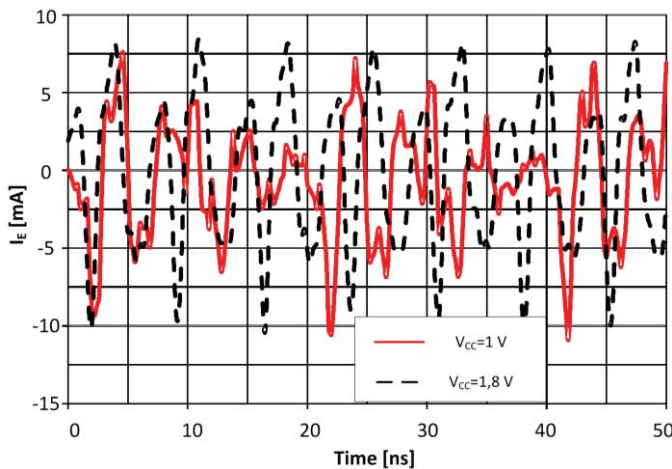


Figure 7: Measurement of the external current.

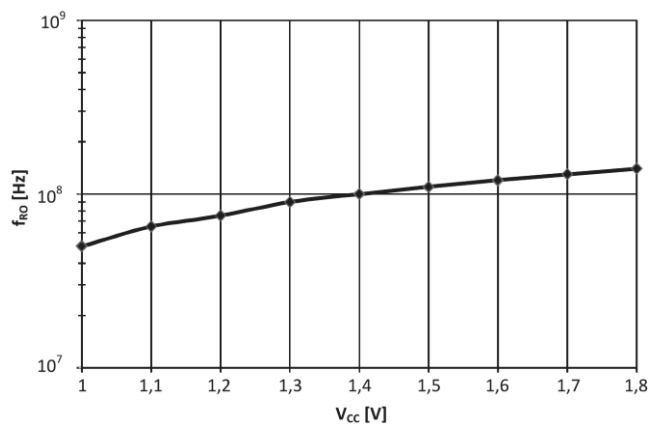


Figure 8: Frequency of the RO for several  $V_{CC}$  voltages.

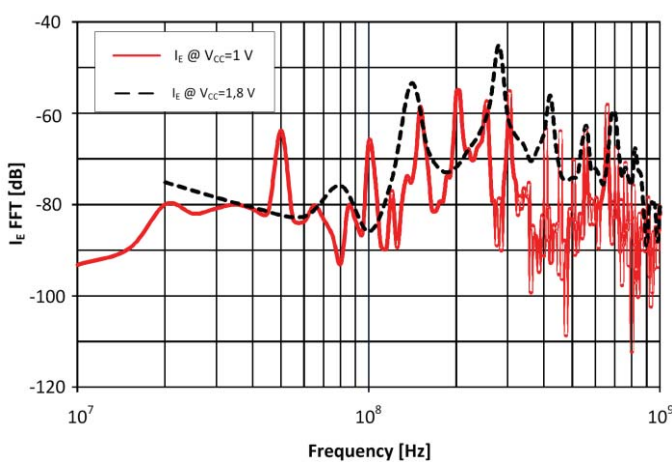


Figure 9: Frequency spectrum of the external current measured.

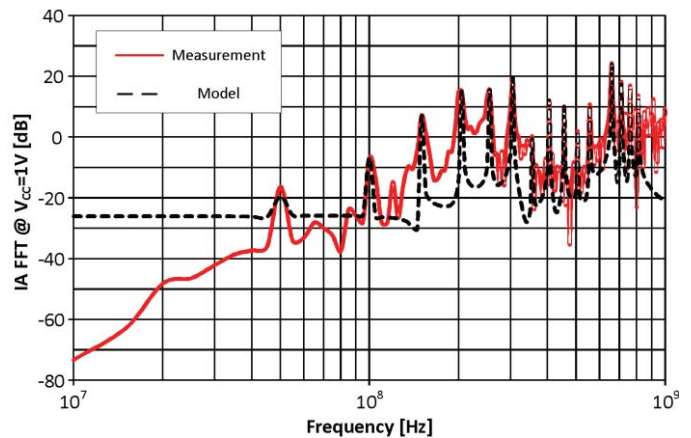


Figure 10: Frequency spectrum of the Internal Activity (Measurements and Model) at  $V_{CC}=1V$

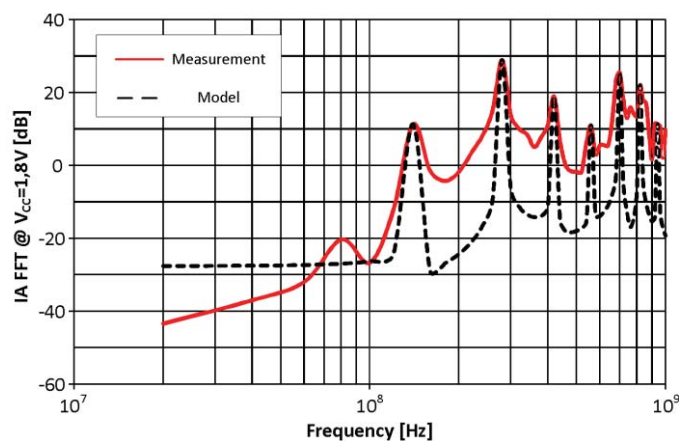


Figure 11: Frequency spectrum of the Internal Activity (Measurements and Model) at  $V_{CC}=1.8V$

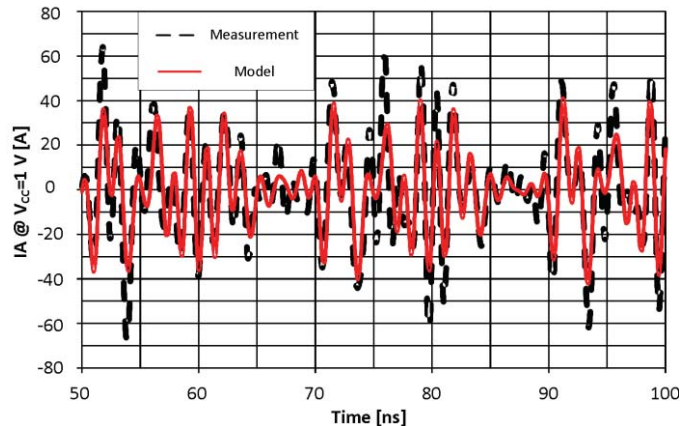


Figure 12: Measurements of Internal Activity and IA new model at  $V_{CC}=1 V$

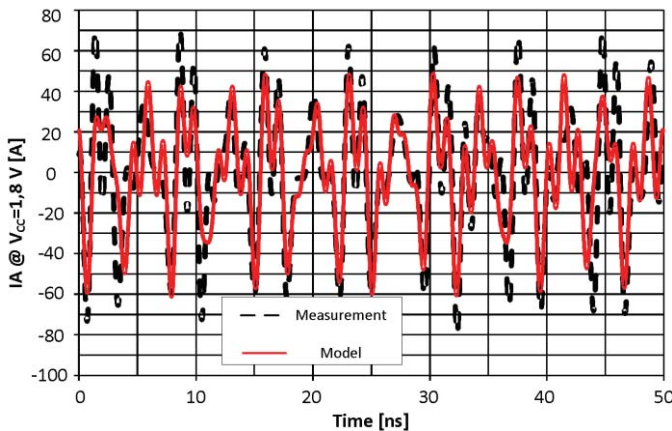


Figure 13: Measurements of Internal Activity and IA new model at  $V_{CC}=1.8$  V

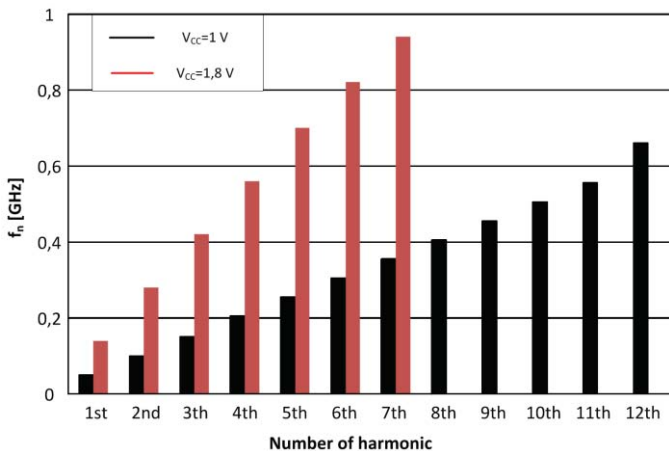


Figure 14: Comparison of the harmonic frequency at different power supply voltages.

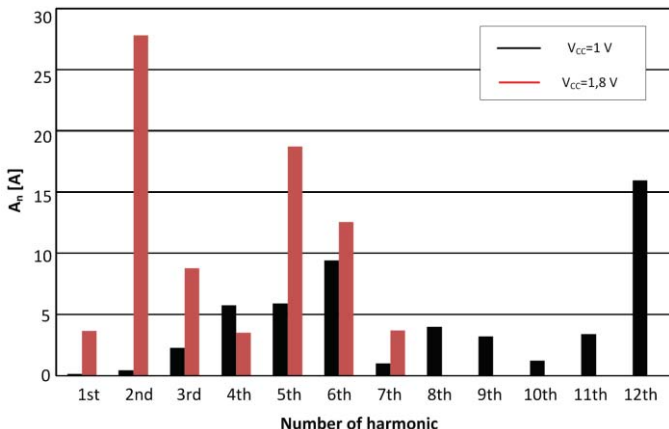


Figure 15: Comparison of the harmonic amplitude at different power supply voltages.

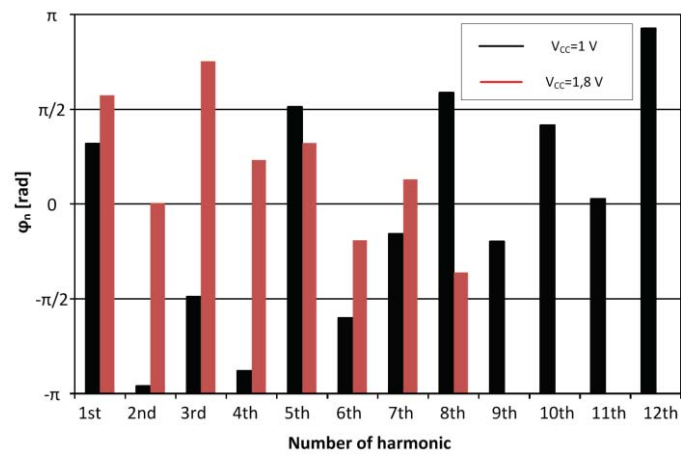


Figure 16: Comparison of the harmonic phase at different power supply voltages.

## V. CONCLUSIONS

This paper presents an alternative approach to model the Internal Activity on the ICEM-CE modeling on the Fourier series expansion up to the N first harmonics, by taking into account the amplitude, frequency and phase. The IA alternative model has been applied in a Ring Oscillator for two different voltages and a good correlation between the measurements and the model has been achieved.

The proposed model can be useful so as to quantify the variations of the IA and model the impact of different factors, as temperature and wear-out mechanisms.

## REFERENCES

- [1] IEC62433-2, Integrated Circuit – EMC IC Modeling – Part 2: Integrated Circuit Emission Model- Conducted Emission.
- [2] Montrose MI. EMC and the Printed Circuit Board: design, theory, and layout made simple. Piscataway, NJ, USA: IEEE Press; 1999
- [3] S. Ben Dhia, M. Ramdani, E. Sicard and J.L. Levant, Electromagnetic compatibility of integrated circuits, Springer (2006).
- [4] T. W. Goodman, H. Fujita, Y. Murakami, and A. T. Murphy, "High speed electrical characterization and simulation of a pin grid array package," IEEE Trans. Compon., Hybrids, Manuf. Technol., vol. 18, no. 1, pp. 163–167, Feb. 1995.
- [5] K. Ichikawa, M. Inagaki, and Y. Sakurai, "Simulation of integrated circuit immunity with LEECS model," in Proc. 17th Int. Zurich Symp. Electromagn. Compat., 2006, pp. 308–311.
- [6] JL Levant, Ch. Marot, M. Meyer and M. Ramdani, "Solving ASIC decoupling with the ICEM-CE Model" in EMC Compo 2009, Toulouse.
- [7] JL Levant; M. Ramdani; R. Perdriau; M. Drissi; , "EMC Assessment at Chip and PCB Level: Use of the ICEM Model for Jitter Analysis in an Integrated PLL," IEEE Transactions on Electromagnetic Compatibility, , vol.49, no.1, pp.182-191, Feb. 2007
- [8] Labussiere-Dorgan, C.; Bendhia, S.; Sicard, E.; Junwu Tao; Quaresma, H.J.; Lochot, C.; Vrignon, B.; , "Modeling the Electromagnetic Emission of a Microcontroller Using a Single Model." IEEE Transactions on Electromagnetic Compatibility, , vol.50, no.1, pp.22-34, Feb. 2008
- [9] Zhou Changlin; Hu Mingxin; Lin Xin; Dang Liming; Yang Tianchi; , "Electromagnetic compatibility analysis and design for digital signal controllers," Electromagnetic Compatibility (APEMC), 2010 Asia-Pacific Symposium on , vol., no., pp.668-671, 12-16 April 2010